A Reconciled Estimate of Glacier Contributions to Sea Level Rise: 2003 to 2009
Alex S. Gardner *et al.*
Science **340**, 852 (2013);
DOI: 10.1126/science.1234532

Source (DLS) and ISIS. We thank C. Tang, J. Parker, and S. Thompson for assistance in using beamline I11 (DLS) and A. Daoud-Aladine for assistance in using the High Resolution Powder Diffractometer (HRPD, ISIS). CCDC 887926 contains the supplementary crystallographic data for this paper. These data can be obtained free of charge via www.ccdc.cam.ac.uk/data_request/cif, by e-mailing data_request@ccdc.cam.ac.uk, or by contacting the Cambridge Crystallographic Data Centre, 12, Union Road, Cambridge CB2 1EZ, UK; fax: +44 1223 336033. We also thank M.S. Islam (Department of Chemistry, University of Bath) for helpful discussion with regards to fitting force-field parameters. Via our membership of the United Kingdom's HPC Materials Chemistry Consortium, which is funded by Engineering and Physical Sciences Research Council (EPSRC) (EP/F067496), this work made use of the facilities of HECToR, the United Kingdom's national high-performance computing service, which is provided by UoEHPCx Limited at the University of Edinburgh, Cray Incorporated and NAG Limited, and funded by the Office of Science and Technology through EPSRC's High End Computing Programme. We thank EPSRC for studentships for C.C. and D.H. M.J.R. is a Royal Society Research Professor.

Supplementary Materials
www.sciencemag.org/cgi/content/full/science.1226558/DC1
Materials and Methods
Supplementary Text
Figs. S1 to S13
Table S1
References (*33–53*)

26 June 2012; accepted 14 March 2013
Published online 11 April 2013;
10.1126/science.1226558

A Reconciled Estimate of Glacier Contributions to Sea Level Rise: 2003 to 2009

Alex S. Gardner,[1,2]* Geir Moholdt,[3] J. Graham Cogley,[4] Bert Wouters,[5,6] Anthony A. Arendt,[7] John Wahr,[5,8] Etienne Berthier,[9] Regine Hock,[7,10] W. Tad Pfeffer,[11] Georg Kaser,[12] Stefan R. M. Ligtenberg,[13] Tobias Bolch,[14,15] Martin J. Sharp,[16] Jon Ove Hagen,[17] Michiel R. van den Broeke,[13] Frank Paul[14]

Glaciers distinct from the Greenland and Antarctic Ice Sheets are losing large amounts of water to the world's oceans. However, estimates of their contribution to sea level rise disagree. We provide a consensus estimate by standardizing existing, and creating new, mass-budget estimates from satellite gravimetry and altimetry and from local glaciological records. In many regions, local measurements are more negative than satellite-based estimates. All regions lost mass during 2003–2009, with the largest losses from Arctic Canada, Alaska, coastal Greenland, the southern Andes, and high-mountain Asia, but there was little loss from glaciers in Antarctica. Over this period, the global mass budget was –259 ± 28 gigatons per year, equivalent to the combined loss from both ice sheets and accounting for 29 ± 13% of the observed sea level rise.

Global estimates of glacier mass changes have traditionally been based on the extrapolation of local geodetic and glaciological measurements. These records indicate increasing mass loss in recent decades (*1–3*). However, a recent study (*4*) using Gravity Recovery and Climate Experiment (GRACE) satellite gravimetry from 2003 to 2010 suggests that global glacier mass wastage is much less than previously thought (*1*, *5*). To investigate this discrepancy, we recalculated existing results from glaciological extrapolation and GRACE to a common spatial and temporal reference that we compare with independent altimetric estimates from the Ice, Cloud, and land Elevation Satellite (ICESat). We provide estimates of regional mass budgets for glaciers peripheral to the Greenland and Antarctic Ice Sheets and for the glaciers of high-mountain Asia (HMA), based on elevation changes from ICESat.

For regional glacier analyses, we relied on the Randolph Glacier Inventory [RGIv3 (*6*)], a globally complete digital database of glacier coverage. It defines 19 glacier regions that contain a total glacierized area of ~729,400 km^2 (circa 2000: Fig. 1 and Table 1). Deriving regional and global mass budgets from glaciological and local geodetic measurements is complicated, because the set of measured glaciers is sparse for many regions and can be biased toward smaller land-terminating glaciers (*7*). Monitoring of glacier mass change on a global scale using satellite gravimetry or altimetry has only become possible with the launch of the GRACE and ICESat satellites in early 2002 and 2003, respectively. The ICESat mission ended in October 2009, giving a 6-year overlap with GRACE from October 2003 to October 2009, during which we are able to compare results from all three methods. Unless otherwise stated, all the mass budgets on which we relied (*8–10*) have been updated to cover this common time span over the RGI regions, with no changes to the original methods. All reported estimates are accompanied by 95% confidence intervals (CIs).

We recalculated recent GRACE glacier mass-change estimates (*4*, *11*) with updated mascons (table S1). We also made alternative GRACE estimates of glacier mass changes by expanding the methods of Wouters *et al*. (*12*), which were originally developed to retrieve mass changes for the Greenland Ice Sheet and Arctic glaciers (*12–14*), to all glacierized regions (table S2). Both analyses use monthly time-variable GRACE gravity-field solutions produced by the University of Texas Center for Space Research: The Wouters *et al*. approach used product Release 5, and the updated Jacob *et al*. estimates (*4*) used product Release 4. The two analyses give a total mass budget for all glaciers outside Greenland and Antarctica of –170 ± 32 Gt year^{-1} and –166 ± 37 Gt year^{-1}, respectively. The two GRACE estimates also agree well on a regional scale (*11*), so for the remaining analysis we averaged them and refer to the combined result as JW12. The averaged gravimetric estimate is half as negative as a more conventional estimate (*2*), based on spatial interpolation of glaciological and local geodetic measurements (hereafter referred to as glaciological records). This method yields a mass budget of –329 ± 121 Gt year^{-1} (we refer to these results as C09). If we include glaciers peripheral to the Greenland and Antarctic Ice Sheets, C09 gives a total estimate for all glaciers of –491 ± 200 Gt year^{-1} which is comparable to an earlier estimate (–402 ± 95 Gt year^{-1}) of glacier mass loss for 2006, also determined from extrapolation of local glaciological records (*1*). Here we address the large discrepancies between gravimetric and glaciological estimates region by region and compare them with estimates from ICESat laser altimetry where available.

Peripheral glaciers in Antarctica (*15*) and Greenland (*16*) account for about 30% of the global glacier area, but until recently there have been no published region-wide estimates for our study period. We present an analysis of elevation changes along ICESat near-repeat tracks, using a plane-fitting technique that accounts for the local surface slope (*8*). We used surface elevations from the GLA12 and GLA06 altimetry products Release 533, with standard saturation correction applied and no correction for potential intercampaign

[1]Graduate School of Geography, Clark University, Worcester, MA 01610, USA. [2]Department of Atmospheric, Oceanic and Space Science, University of Michigan, Ann Arbor, MI 48109, USA. [3]Institute of Geophysics and Planetary Physics, Scripps Institution of Oceanography, La Jolla, CA 92093, USA. [4]Department of Geography, Trent University, Peterborough, Ontario K9J 7B8, Canada. [5]Department of Physics, University of Colorado at Boulder, Boulder, CO 80309, USA. [6]Bristol Glaciology Centre, School of Geographical Science, Bristol BS8 1SS, UK. [7]Geophysical Institute, University of Alaska Fairbanks, Fairbanks, AK 99775, USA. [8]Cooperative Institute for Research in Environmental Sciences, University of Colorado at Boulder, Boulder, CO 80309, USA. [9]Centre National de la Recherche Scientifique, Université de Toulouse, LEGOS, 14 Avenue E. Belin, 31400 Toulouse, France. [10]Department of Earth Sciences, Uppsala University, SE-751 05 Uppsala, Sweden. [11]Institute of Arctic and Alpine Research, University of Colorado at Boulder, Boulder, CO 80309, USA. [12]Institute of Meteorology and Geophysics, Universität Innsbruck, A-6020 Innsbruck, Austria. [13]Utrecht University, Institute for Marine and Atmospheric Research Utrecht, 3508 TA Utrecht, Netherlands. [14]Department of Geography, University of Zurich, CH-8057 Zurich, Switzerland. [15]Institut für Kartographie, Technische Universität Dresden, D-01062 Dresden, Germany. [16]Department of Earth and Atmospheric Sciences, University of Alberta, Edmonton, Alberta T6G 2E3, Canada. [17]Department of Geosciences, University of Oslo, Box 1047 Blindern, N-0316, Oslo, Norway.

*Corresponding author. E-mail: agardner@clarku.edu

biases (*11*). In Antarctica, we corrected elevation changes for variations due to change in the firn density, using a firn pack model with a horizontal resolution of ~27 km (*17*, *18*). We attributed residual volume changes after these firn corrections to changes in glacier ice and converted them to mass changes, using a density of 900 ± 17 kg m^{-3}. The Antarctic peripheral glaciers (133,200 km^2) have not changed much in total mass (–6 ± 10 Gt $year^{-1}$), which is in contrast to earlier modeling estimates for 1961–2004 (*19*). There are, however, subregional examples of both loss (Antarctic Peninsula Islands, –7 ± 4 Gt $year^{-1}$) and gain (Ellsworth Land Islands, 3 ± 4 Gt $year^{-2}$). For Greenland we lack firn pack model simulations and instead rely on estimates of the firn area and the bulk density of the firn volume change (*11*). We estimate a total mass budget of –38 ± 7 Gt

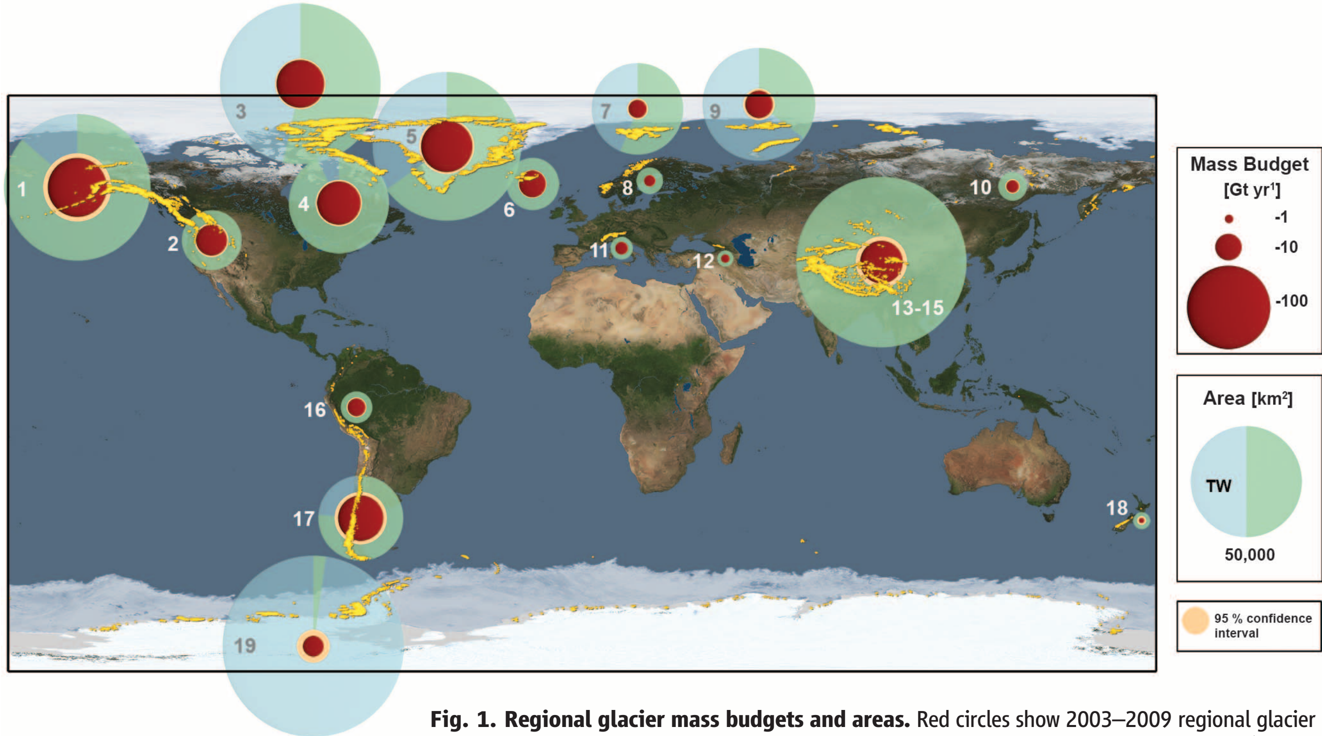

Fig. 1. Regional glacier mass budgets and areas. Red circles show 2003–2009 regional glacier mass budgets, and pale blue/green circles show regional glacier areas with tidewater basin fractions (the extent of ice flowing to termini in the ocean) in blue shading (Table 1). Peach-colored halos surrounding red circles show the 95% CI in mass change estimates, but can only be seen in regions that have large uncertainties.

Table 1. Regional areas and mass budgets. Regional breakdown of total and tidewater glacier basin area, best estimate of mass budget for 2003–2009 with the 95% CI, and methods selected as most suitable for estimating glacier mass change. G, GRACE; I, ICESat; gl, glaciological.

	Region	Total area (km^2)	Tidewater area (km^2)	Mass budget (kg m^{-2} $year^{-1}$)	Mass budget (Gt $year^{-1}$)	Method	Ref.
1	Alaska	87,100	11900	−570 ± 200	−50 ± 17	G	New, (*4*, *9*, *10*)
2	Western Canada/United States	14,600	0	−930 ± 230	−14 ± 3	gl	(*2*)
3	Arctic Canada north	104,900	48,800	−310 ± 40	−33 ± 4	I, G	New, (*4*, *13*)
4	Arctic Canada south	40,900	3,000	−660 ± 110	−27 ± 4	I, G	New, (*4*, *13*)
5	Greenland	89,700	31,300	−420 ± 70	−38 ± 7	I	New
6	Iceland	11,100	0	−910 ± 150	−10 ± 2	G, gl	New, (*2*, *4*)
7	Svalbard	34,000	14,900	−130 ± 60	−5 ± 2	I, G	New, (*4*, *8*)
8	Scandinavia	2,900	0	−610 ± 140	−2 ± 0	gl	(*2*)
9	Russian Arctic	51,600	33,400	−210 ± 80	−11 ± 4	I, G	New, (*4*, *14*)
10	North Asia	3,400	0	− 630 ± 310	−2 ± 1	gl	(*2*)
11	Central Europe	2,100	0	−1060 ± 170	−2 ± 0	gl	(*2*)
12	Caucasus and Middle East	1,100	0	−900 ± 160	−1 ± 0	gl	(*2*)
13–15	HMA	118,200	0	−220 ± 100	−26 ± 12	I, G	New, (*4*)
16	Low latitudes	4,100	0	−1080 ± 360	−4 ± 1	gl	(*2*)
17	Southern Andes	29,400	7,000	−990 ± 360	−29 ± 10	G	New, (*4*, *25*)
18	New Zealand	1,200	0	−320 ± 780	0 ± 1	gl	(*2*)
19	Antarctic and sub–Antarctic	133,200	130,200	−50 ± 70	−6 ± 10	I	New
Total, excluding Greenland and Antarctic		506,600	119,000	−420 ± 50	−215 ± 26		
Global total		729,400	280,500	−350 ± 40	−259 ± 28		

year^{-1} for the Greenland peripheral glaciers (89,700 km^2). All subregions experienced significant thinning [Fig. 2 (*11*)], except for the Flade Isblink Ice Cap, Greenland's largest ice cap (*20*). Our estimate is consistent with a recently published estimate of –28 ± 11 Gt year^{-1} for the period 2003–2008 that was determined from ICESat data using methods comparable to ours but assuming a larger firn area and lower bulk density for the firn volume change (*21*). We do not include this estimate in our analysis, as it does not cover the full 2003–2009 period. ICESat-based estimates are less negative than C09 in both Greenland and Antarctica (Fig. 3), but only significantly different in Antarctica, where the C09 estimate is 100 Gt year^{-1} more negative. The cause of the disagreement is discussed after our assessment of regional mass changes.

Outside of Greenland and Antarctica, there are four high-latitude regions with published glacier mass budgets from ICESat (2003–2009) that we can compare with the C09 and JW12 estimates: Arctic Canada north (*13*) (–37 ± 7 Gt year^{-1}), Arctic Canada south (*13*) (–24 ± 6 Gt year^{-1}), Svalbard (*8*) (–5 ± 1 Gt year^{-1}), and the Russian Arctic (*14*) (–10 ± 4 Gt year^{-1}). Summing mass budgets for these four regions gives an ICESat estimate of –75 ± 10 Gt year^{-1}, a JW12 estimate of –78 ± 12 Gt year^{-1}, and a C09 estimate of –116 ± 52 Gt year^{-1}. Regional errors are considered uncorrelated for ICESat and JW12, but fully correlated for C09. ICESat and GRACE agree well in all regions, whereas C09 is considerably more negative, although error bounds usually overlap [Fig. 3 (*11*)].

The two remaining large (>5000 km^2) high-latitude regions, Alaska and Iceland, have no published mass budgets from ICESat. Alaska mass-budget estimates from C09 and JW12 are –72 ± 22 Gt year^{-1} and –42 ± 11 Gt year^{-1}, and two other GRACE estimates give mass budgets of –54 ± 26 Gt year^{-1} and –61 ± 22 Gt year^{-1} (*9*, *10*). Although estimates have overlapping error bounds, there is still considerable spread in the mean values. For Iceland, the C09 and JW12 estimates of glacier mass change of –9 ± 2 Gt year^{-1} and –11 ± 3 Gt year^{-1} agree well.

The largest glacierized region outside the Arctic and Antarctic is HMA. Glacier changes in this region are spatially heterogeneous and not well known (*22*). Himalayan and Hindu Kush glaciers have recently been found to be losing mass (*23*), whereas the glaciers in the Karakoram are in near balance (*24*). For complete comparison with JW12 and C09, we analyzed ICESat altimetry for

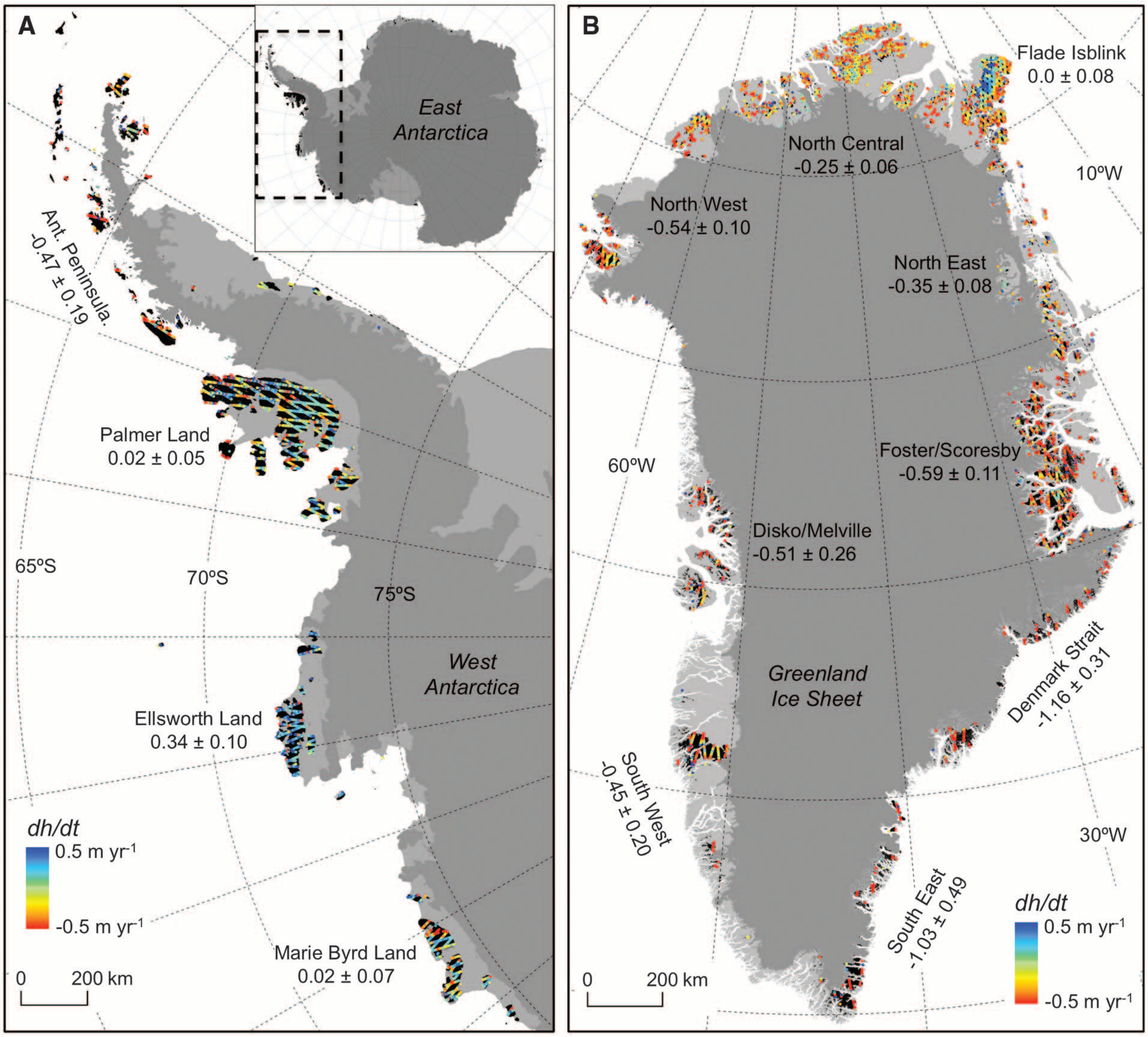

Fig. 2. Elevation changes for glaciers peripheral to the ice sheets. Elevation change rates (*dh/dt*) between October 2003 and October 2009 for peripheral glaciers in (**A**) West Antarctica and (**B**) Greenland. Gray shadings from black to white show glaciers, ice sheets, ice shelves, land surfaces, and ocean, respectively. West Antarctica contains 85% of the peripheral glacier cover in Antarctica. The remaining glaciers are found on scattered islands around East Antarctica (11%, inset map) and on remote sub-Antarctic islands (4%, not shown). Text labels define a set of subregions with accompanying average elevation change rates in m year^{-1} (table S4). Uncertainties give the 95% CI.

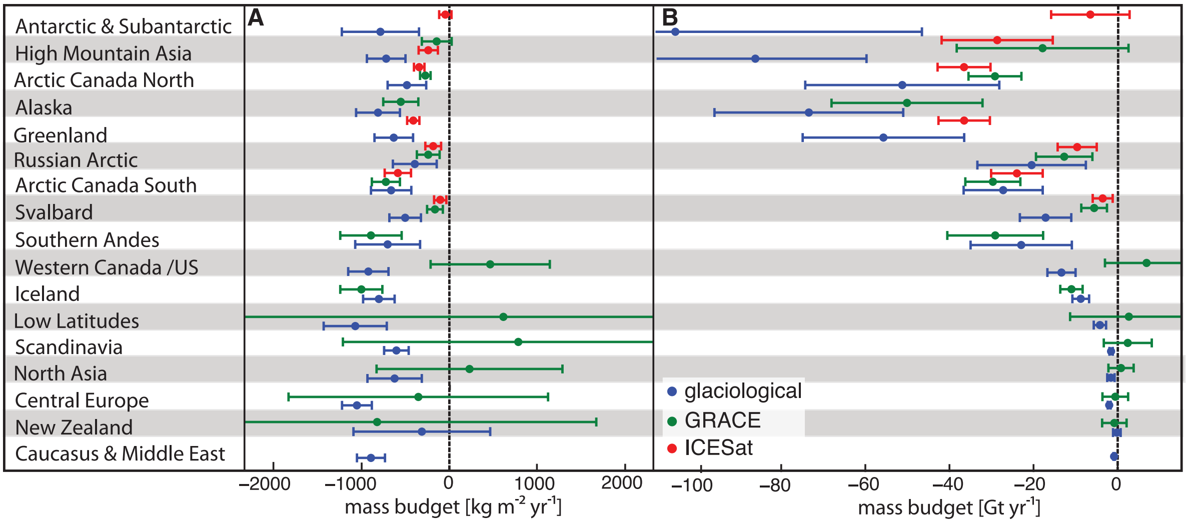

Fig. 3. Comparison of regional glacier mass-budget estimates. Regional estimates of glacier mass change for 2003–2009 in (**A**) kg m^{-2} year^{-1} and (**B**) Gt year^{-1}. Estimates are as assessed by ICESat (*8*, *13*, *14*) and GRACE []W12 (*9*, *10*)] and from interpolation of glaciological records (*2*) with an updated measurement data set for 2003–2009 (glaciological). Regions are arranged from top to bottom by total glacierized area. Uncertainties give the 95% CI.

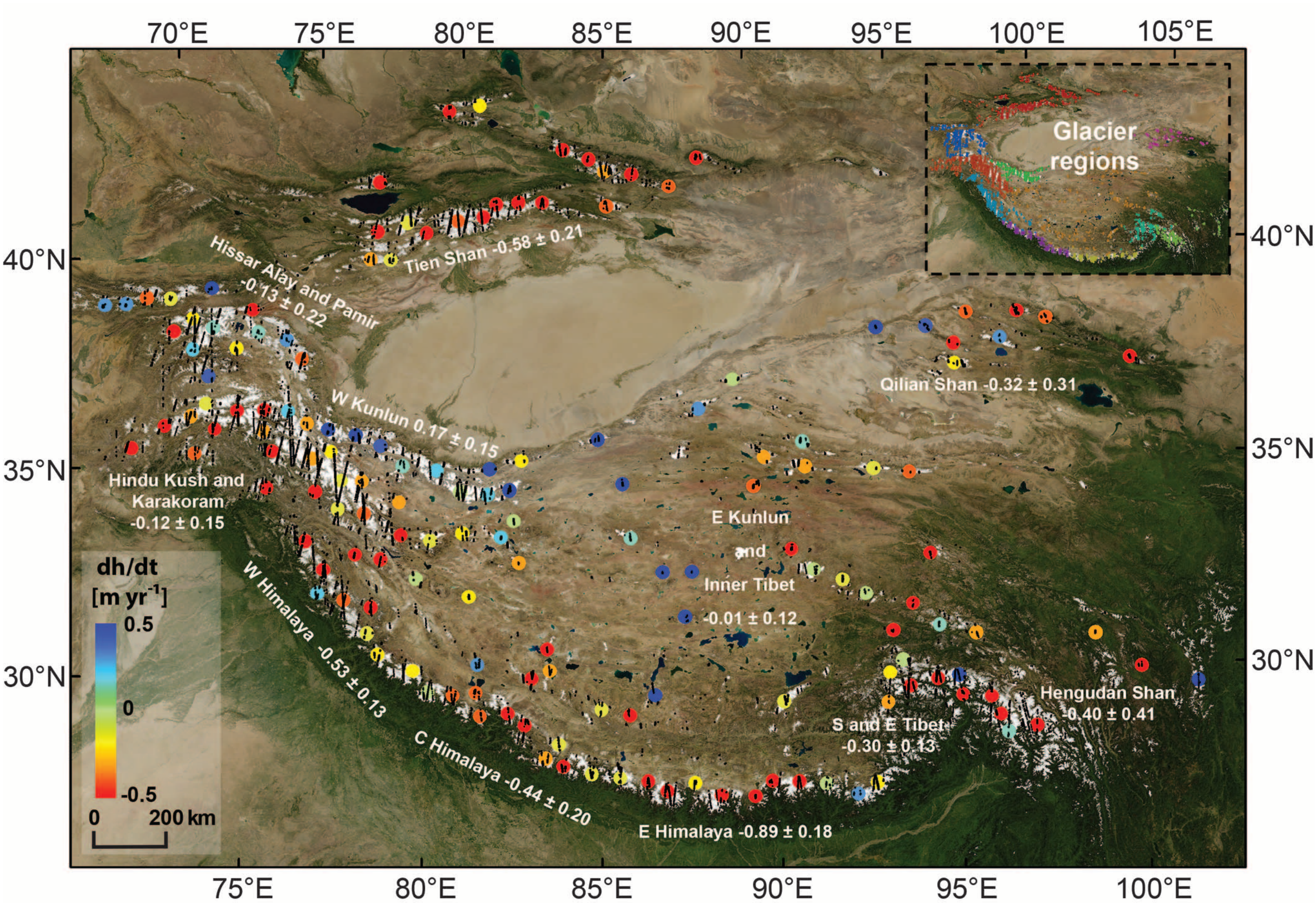

Fig. 4. Elevation changes for high-mountain Asia glaciers. Averaged elevation change rates (*dh*/*dt*) between October 2003 and October 2009 for high-mountain Asia. Each colored dot represents an independent spatial average of a minimum of 50 *dh*/*dt* observations within a radius of 50 km. ICESat ground tracks over glaciers are shown with thin black lines. The inset image and text labels define a set of subregions for which we have estimated area-averaged elevation changes (shown here in m year^{-1} together with their uncertainties) and mass budgets (table S5). Uncertainties give the 95% CI.

the entire HMA using two approaches: a modification of the method of Moholdt and others (*8*); and methods similar to those of Kääb and others (*23*), whose analysis was restricted to about half of the glacierized area in HMA (*11*). Both approaches use an elevation model from the Shuttle Radar Topography Mission to correct for topographic differences between ICESat points. The results confirm a heterogeneous pattern of elevation change [Fig. 4 (*11*)], with most rapid thinning (<–0.4 m year^{-1}) in the south (Himalaya) and north (Tien Shan), moderate rates of thinning (~ –0.3 m year^{-1}) in eastern and southern Tibet, and near balance (–0.12 to +0.16 m year^{-1}) in the western and central portions of the region (Pamir, Karakoram, and western Kunlun). We converted volume changes to mass changes using a density of 900 kg m^{-3} and summed the subregional estimates (table S5) to obtain a total HMA mass budget of –29 ± 13 Gt year^{-1}. This estimate shows significant mass loss and is within the error bounds of JW12 (–19 ± 20 Gt year^{-1}). Both satellite-based estimates are significantly less negative than C09 (–86 ± 26 Gt year^{-1}).

The two remaining large (>5000 km^2) glacierized regions are the southern Andes (including Patagonia) and western Canada/United States. For the southern Andes, the mass-budget estimates of JW12 (–29 ± 10 Gt year^{-1}) and C09 (–21 ± 11 Gt year^{-1}) agree relatively well with another GRACE estimate (–26 ± 12 Gt year^{-1}: 2003–2009) (*25*) and with estimates for a longer time period from the analysis of multitemporal digital elevation models for the three major icefields in the region (–28 ± 3 Gt year^{-1}: 2000–2011/12) (*26*–*28*). The comparison is more troublesome in western Canada/United States, where C09 gives a net loss of –14 ± 3 Gt year^{-1} and JW12 gives a net gain of +7 ± 10 Gt year^{-1}. The only previous estimate (*29*) of glacier mass change for this region, based on differencing of digital elevation models, yielded mass loss at –8 ± 4 Gt year^{-1} during 1985–2000 (excluding subregions that are part of the Alaska region as defined by RGI). The C09 estimate for the same period (–9 ± 2 Gt year^{-1}) agrees well with Schiefer and others (*29*), and glaciological records indicate that the most recent decade has seen accelerated glacier loss. This suggests that C09 performs satisfactorily in this region and that JW12 may not adequately separate the glacier mass signal from other mass changes in the region.

The remaining six small regions (glacier area <5000 km^2 each) contain only 2% of Earth's glaciers by area (Table 1). The JW12 gravimetric estimates of glacier mass change for these regions have larger uncertainties than the glaciological estimates (Fig. 3), and there are no concurrent regional-scale measurements of elevation changes, because ICESat track coverage is insufficient for reliable estimation. These sparsely glacierized regions all have a relatively high density of glaciological records (table S3), and we therefore expect C09 to perform satisfactorily here. Summing all six regions gives a C09 estimate of –12 ± 4 Gt year^{-1} and a JW12 estimate of +4 ± 16 Gt year^{-1}.

Our assessment shows that ICESat and GRACE estimates of mass change for large glacierized regions agree well and that estimates derived from the interpolation of glaciological records can be substantially more negative (Fig. 3). This suggests that the database of glaciological records is negatively biased. To investigate this bias, we extracted subsamples of ICESat elevation change data within 100 km of the C09 glaciological measurements in the five regions where both data sets are available. These ICESat subsamples reveal that the neighborhoods of the glaciological measurements are typically thinning more rapidly than the regional mean (Fig. 5). Forty-one of the 49 glacier neighborhoods had rates of thinning higher than their respective regional averages (fig. S9). Across the five regions, which account for 75% of the global glacierized area, the area-weighted difference between the regional mean and the elevation changes in the C09 neighborhoods is –0.43 m year^{-1}, which would translate to a large global mass-budget bias of –201 Gt year^{-1} for 2003–2009. Thus, glaciers with glaciological measurements tend to be located in subregions where mass loss is greater than in their region as a whole, and this sampling bias is probably the major source of the discrepancy between C09 and the satellite-based estimates.

For our consensus estimate of global glacier mass wastage, GRACE and ICESat estimates are favored for all regions that have glacierized area greater than 5000 km^2, except western Canada/United States. In the latter region, and in six smaller regions where the density of in situ measurements is relatively high and the GRACE uncertainty exceeds ±1000 kg m^{-2} year^{-1}, we take C09 as the best estimate of mass change. C09 also has a relatively high measurement density for Iceland, so we included it in the method-averaged estimate for Iceland. On the basis of this synthesis, we estimate that Earth's glaciers had a mass budget for 2003–2009 of –215 ± 26 Gt year^{-1} when peripheral glaciers in Greenland and Antarctica are excluded, and –259 ± 28 Gt year^{-1} when peripheral glaciers are included (Table 1).

Compared to longer-term global estimates from 1960–1961 to 2004–2005, our consensus mass budget is slightly less negative than three of four previous studies (*2*, *19*, *30*) but more negative than the fourth (*3*). This could imply that there has been no increase in glacier mass loss in the most recent decade, but this conflicts with the glaciological records themselves (Fig. 6) and with repeat geodetic measurements (*13*, *25*, *31*–*33*).

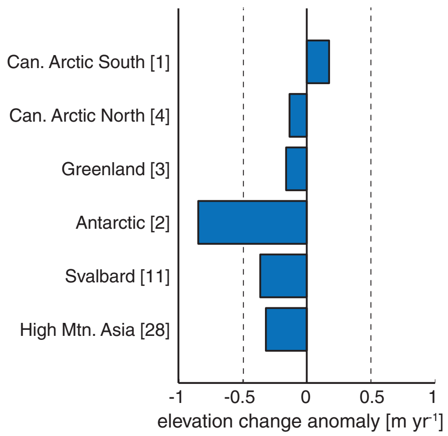

Fig. 5. Possible bias due to sparse spatial coverage of glaciological records. ICESat-derived elevation change anomalies between neighborhoods of glaciological and local geodetic measurements and averages over their RGI regions. Each neighborhood is centered on a measured glacier and has a radius of 100 km. Each region name is followed by its number of measured glaciers during the 2003–2009 period. Negative values indicate that neighborhoods of glaciological records experienced thinning at higher rates than the regional average.

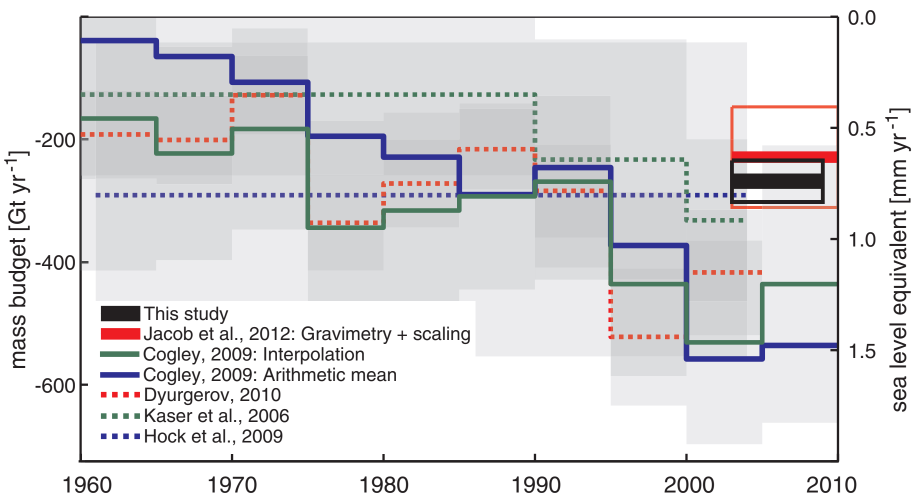

Fig. 6. Global estimates of glacier mass change. All estimates have been multiplied by the ratio of the total glacier area used in this study, 729,400 km^2, to that used in each source. 95% CIs are shown for all estimates except the arithmetic averages of C09 (*2*), which have formal errors in the range from 410 to 1520 Gt year^{-1}. The two C09 estimates are determined from an updated set of glaciological records using the methods of Cogley (*2*).

We instead suggest that most previous assessments have overestimated global mass losses because of the interpolation of sparse glaciological measurements that are not representative for the largest glacierized regions. We can only demonstrate this negative bias for the 2003–2009 period, but it has long been suspected for earlier periods as well (*34*, *35*). This calls for a reexamination of previous global estimates based on the interpolation of glaciological records, which will probably lead to a downward revision of the estimated total contribution of glaciers to sea level rise over the past century.

Our consensus estimate of glacier mass wastage between 2003 and 2009 implies a sea-level contribution of 0.71 ± 0.08 mm of sea-level equivalent (SLE) year^{-1}, accounting for 29 ± 13% of the observed sea-level rise (2.50 ± 0.54 mm year^{-1}) for the same period (*11*). The total glacier mass loss is comparable to a recent estimate for the whole of Greenland and Antarctica (*36*) (peripheral glaciers + ice sheets) for the period 2003–2008. To avoid double counting, we subtracted our estimates for peripheral glacier mass loss from this total to obtain a total ice-sheet mass budget of −290 ± 50 Gt year^{-1} (*11*) and a total land ice (all glaciers + ice sheets) mass budget of −549 ± 57 Gt year^{-1}, amounting to a sea-level rise of 1.51 ± 0.16 mm of SLE year^{-1}, which is 61 ± 19% of the total global sea-level rise (*11*).

References and Notes

1. M. F. Meier *et al*., *Science* **317**, 1064 (2007).
2. J. G. Cogley, *Ann. Glaciol.* **50**, 96 (2009).
3. G. Kaser, J. G. Cogley, M. B. Dyurgerov, M. F. Meier, A. Ohmura, *Geophys. Res. Lett.* **33**, L19501 (2006).
4. T. Jacob, J. Wahr, W. T. Pfeffer, S. Swenson, *Nature* **482**, 514 (2012).
5. J. A. Church *et al*., *Geophys. Res. Lett.* **38**, L18601 (2011).
6. A. Arendt *et al*., *Randolph Glacier Inventory: A Dataset of Global Glacier Outlines Version: 2.0* (Global Land Ice Measurements from Space, Digital Media, Boulder, CO, 2012).
7. M. Zemp, M. Hoelzle, W. Haeberli, *Ann. Glaciol.* **50**, 101 (2009).
8. G. Moholdt, C. Nuth, J. O. Hagen, J. Kohler, *Remote Sens. Environ.* **114**, 2756 (2010).
9. I. Sasgen, V. Klemann, Z. Martinec, *J. Geodyn.* **59–60**, 49 (2012).
10. S. B. Luthcke, A. A. Arendt, D. D. Rowlands, J. J. McCarthy, C. F. Larsen, *J. Glaciol.* **54**, 767 (2008).
11. Materials and methods are available in the supplementary materials on *Science* Online.
12. B. Wouters, D. Chambers, E. J. O. Schrama, *Geophys. Res. Lett.* **35**, L20501 (2008).
13. A. S. Gardner *et al*., *Nature* **473**, 357 (2011).
14. G. Moholdt, B. Wouters, A. S. Gardner, *Geophys. Res. Lett.* **39**, L10502 (2012).
15. A. Bliss, R. Hock, J. G. Cogley, *Ann. Glaciol.* **54**, 191 (2013).
16. P. Rastner *et al*., *Cryosphere* **6**, 1483 (2012).
17. H. D. Pritchard *et al*., *Nature* **484**, 502 (2012).
18. S. R. M. Ligtenberg, M. M. Helsen, M. R. van den Broeke, *Cryosphere* **5**, 809 (2011).
19. R. Hock, M. de Woul, V. Radić, M. Dyurgerov, *Geophys. Res. Lett.* **36**, L07501 (2009).
20. E. J. Rinne *et al*., *J. Geophys. Res.* **116**, F03024 (2011).
21. T. Bolch *et al*., *Geophys. Res. Lett.* **40**, 875 (2013).
22. T. Bolch *et al*., *Science* **336**, 310 (2012).
23. A. Kääb, E. Berthier, C. Nuth, J. Gardelle, Y. Arnaud, *Nature* **488**, 495 (2012).
24. J. Gardelle, E. Berthier, Y. Arnaud, *Nat. Geosci.* **5**, 322 (2012).
25. E. R. Ivins *et al*., *J. Geophys. Res.* **116**, B02403 (2011).
26. M. J. Willis, A. K. Melkonian, M. E. Pritchard, J. M. Ramage, *Remote Sens. Environ.* **117**, 184 (2012).
27. M. J. Willis, A. K. Melkonian, M. E. Pritchard, A. Rivera, *Geophys. Res. Lett.* **39**, L17501 (2012).
28. A. K. Melkonian *et al*., *Cryosphere Discuss.* **6**, 3503 (2012).
29. E. Schiefer, B. Menounos, R. Wheate, *Geophys. Res. Lett.* **34**, L16503 (2007).
30. M. Dyurgerov, M. F. Meier, R. L. Armstrong, *Mass Balance of Mountain and Sub-Polar Glaciers Outside the Greenland and Antarctic ice sheets: Supplement to Occasional Paper No. 55* (Institute of Arctic and Alpine Research, University of Colorado, Boulder, CO, 2005).
31. E. Berthier, E. Schiefer, G. K. C. Clarke, B. Menounos, F. Remy, *Nat. Geosci.* **3**, 92 (2010).
32. E. Rignot, A. Rivera, G. Casassa, *Science* **302**, 434 (2003).
33. A. S. Gardner, G. Moholdt, A. Arendt, B. Wouters, *Cryosphere* **6**, 1103 (2012).
34. M. B. Dyurgerov, M. F. Meier, *Arct. Alp. Res.* **29**, 379 (1997).
35. J. G. Cogley, W. P. Adams, *J. Glaciol.* **44**, 315 (1998).
36. A. Shepherd *et al*., *Science* **338**, 1183 (2012).

Acknowledgments: We thank K. Matsuo, M. Huss, T. Jacob, A. Kääb, S. Luthcke, A. Willsman, M. Willis, and I. Sasgen for updated or early access to regional estimates of glacier mass change; M. Flanner, T. Jacob, and S. Swenson for helping with analysis of the hydrologic models; A. Bliss, N. Mölg, C. Nuth, P. Rastner, M. Willis, and G. Wolken for providing regional areas of ocean-terminating glacier basins; J. Lenaerts and J. van Angelen for providing RACMO2 output for Greenland and Antarctica; J. Box and C. Chen for making available Greenland Ice Sheet snowline estimates; G. A, R. Riva, and P. Stocchi for providing glacial isostatic adjustment models; and C. Starr and the NASA/Goddard Space Flight Center Scientific Visualization Studio for help with Fig. 1. This work was supported by funding to A.S.G. and M.J.S. from the Natural Sciences and Engineering Research Council of Canada, G.M. from NASA award NNX09AE52G, B.W. from a Marie Curie International Outgoing Fellowship within the 7th European Community Framework Programme (FP7-PEOPLE-2011-IOF-301260), E.B. from the TOSCA program of the French Space Agency (CNES), R.H. from NASA grants NNX11AF41G and NNX11A023G and NSF grant ANT-1043649, G.K. from Austrian Science Fund (FWF) grant P25362-N26, T.B. from the Deutsche Forschungsgemeinschaft (DFG, BO 3199/2-1), and F.P. from European Space Agency project Glaciers_cci (4000101778/10/I-AM).

Supplementary Materials
www.sciencemag.org/cgi/content/full/340/6134/852/DC1
Materials and Methods
Figs. S1 to S10
Tables S1 to S5
References

26 December 2012; accepted 7 March 2013
10.1126/science.1234532

Inhibition of PRC2 Activity by a Gain-of-Function H3 Mutation Found in Pediatric Glioblastoma

Peter W. Lewis,[1] Manuel M. Müller,[2] Matthew S. Koletsky,[1] Francisco Cordero,[3] Shu Lin,[4] Laura A. Banaszynski,[1] Benjamin A. Garcia,[4] Tom W. Muir,[2] Oren J. Becher,[3] C. David Allis[1]*

Sequencing of pediatric gliomas has identified missense mutations Lys27Met (K27M) and Gly34Arg/Val (G34R/V) in genes encoding histone H3.3 (*H3F3A*) and H3.1 (*HIST3H1B*). We report that human diffuse intrinsic pontine gliomas (DIPGs) containing the K27M mutation display significantly lower overall amounts of H3 with trimethylated lysine 27 (H3K27me3) and that histone H3K27M transgenes are sufficient to reduce the amounts of H3K27me3 in vitro and in vivo. We find that H3K27M inhibits the enzymatic activity of the Polycomb repressive complex 2 through interaction with the EZH2 subunit. In addition, transgenes containing lysine-to-methionine substitutions at other known methylated lysines (H3K9 and H3K36) are sufficient to cause specific reduction in methylation through inhibition of SET-domain enzymes. We propose that K-to-M substitutions may represent a mechanism to alter epigenetic states in a variety of pathologies.

Somatic mutations in genes encoding proteins that modify chromatin dynamics frequently contribute to tumorigenesis (*1*). Mutations in subunits of the Polycomb repressive complex 2 (PRC2) are often associated with tumor progression (*2*). PRC2 normally helps maintain epigenetic gene silencing and X chromosome inactivation through enzymatic di- and trimethylation of K27 on histone H3 (*3*). In addition to enzymatic machinery, histone H3 missense mutations in pediatric gliomas represent direct evidence that alterations of the histones themselves can promote cancer. In two pediatric brain cancers, diffuse intrinsic pontine gliomas (DIPGs) and supratentorial glioblastoma multiforme (GBMs), 60% of patients studied exhibited one of two mutually exclusive mutations in either *H3F3A*, one of two genes encoding the histone H3 variant H3.3, or *HIST1H3B*, one of several genes encoding H3.1 (*4*–*6*). The K27M mutation occurring in either *H3F3A* or *HIST1H3B* was observed in nearly 80% of DIPGs, and 22% of non–brain stem gliomas (*6*).

We sought to determine whether DIPG samples that contain the K27M mutation exhibit global changes in key regulatory histone modifications. Immunoblots with antisera raised against the K27M substitution (fig. S1A) indicated the presence of

[1]Laboratory of Chromatin Biology and Epigenetics, The Rockefeller University, New York, NY 10065, USA. [2]Department of Chemistry, Princeton University, Princeton, NJ 08544, USA. [3]Departments of Pediatrics and Pathology, Preston Robert Tisch Brain Tumor Center, Duke University Medical Center, Durham, NC 27710, USA. [4]Department of Biochemistry and Biophysics, Perelman School of Medicine, University of Pennsylvania, Philadelphia, PA 19104, USA.

*Corresponding author. E-mail: alliscd@rockefeller.edu